IAC–24–IAC-24,C4,4,8,x86883

Green Solid Fuels with Enhanced Mechanical Properties: Sustainable Waxes and Scale-up Analysis of Armored Grains

Christian Paravan[a*], Alam U. Garcidueñas Correa[b], Vincenzo Pagliacci[c], Federico Giambelli[d], Riccardo Bisin[e]

[a] *Department of Aerospace Science and Technology, Politecnico di Milano, via LaMasa 34, 20156, Milan, Italy, christian.paravan@polimi.it*
[b] *Faculty of Aerospace Engineering - Sustainable Aircraft Propulsion, TU Delft, Kluyverweg 1, 2629, HS Delft, Netherlands, a.u.garciduenascorrea@tudelft.nl*
[c] *Department of Aerospace Science and Technology, Politecnico di Milano, via LaMasa 34, 20156, Milan, Italy, vincenzo.pagliacci@mail.polimi.it*
[d] *Department of Aerospace Science and Technology, Politecnico di Milano, via LaMasa 34, 20156, Milan, Italy, federico.giambelli@polimi.it*
[e] *Department of Aerospace Science and Technology, Politecnico di Milano, via LaMasa 34, 20156, Milan, Italy, riccardo.bisin@polimi.it*
[*] *Corresponding author*

Abstract

Implementation of hybrid rocket engines in launch systems is hampered by the slow fuel regression rate, in turn implying reduced thrust levels. The most promising solutions for achieving fast regression rates with simple fuel grain geometries are (i) the use of liquefying formulations and (ii) non-conventional oxidizer injection methods. However, the ballistic performance advantages of liquefying fuels are limited by their low mechanical strength. Recently, new reinforcing strategies for liquefying fuels have emerged thanks to 3D printing technology. These innovations include the *armored grain* a heterogeneous fuel. In the armored grain, a 3D-printed cellular structure is embedded in a liquefying fuel matrix. The cellular structure is a reinforcing element, while the liquefying fuel (typically, a wax) provides fast burning behavior. This paper discusses lab-scale testing of wax-based armored grains through pre-burning analysis and combustion testing. It also explores the use of liquefying fuels from sustainable sources and presents the scale-up of the armored grain technology. With standard flow injection, armored grains achieve significantly faster regression rates than pure paraffin wax, with up to a 90% increase under reference conditions. This increased burning performance is paired with enhanced mechanical properties. Under the tested conditions, at lab-scale, grains with embedded cellular structures maintain fast regression rates regardless of the injection method used (standard/swirl). The scalability of the armored grain solution is demonstrated using a test bench developed by Skyward Experimental Rocketry, a student association at the Politecnico di Milano.

Nomenclature

Symbols

Δt_b	=	Burning time (from pressure trace), s
ϵ_y	=	Strain at Yield, %
λ	=	Gyroid unit cell length, mm
$\tilde{\rho}_{\%}$	=	Percent relative density of a structure, %
ρ_f	=	Solid fuel density, kg/m^3
σ_y	=	Stress at yield, MPa
a_r	=	Pre-exponential factor, $(mm/s)/[kg/(m^2 s)]^{n_r}$
$D(t)$	=	Central port diameter (at a given time), mm
D_e	=	External grain diameter, mm
E	=	Compressive elastic modulus, MPa
G_{ox}	=	Oxidizer mass flux, $kg/(m^2 s)$
n_r	=	Exponent
p_c	=	Combustion chamber pressure, MPa
r_f	=	Solid fuel regression rate, mm/s
T	=	Temperature, K

Acronyms/Abbreviations

ABS	=	Acrylonitrile Butadiene Styrene
DTA	=	Differential Thermal Analysis (DTA)
GY	=	Gyroid
HRE	=	Hybrid Rocket Engine
MB	=	Mass-Based regression rate data
mWP	=	Micro-crystalline paraffin wax
SPLab	=	Space Propulsion Laboratory
sWB	=	Sustainable Wax (type B)
sWC	=	Sustainable Wax (type C)
TG	=	Thermogravimetry

1. Introduction

More sustainable, greener and low-recurring cost propulsion is renewing the interest in HREs for launch applications. Worldwide, startups are pursuing projects on HREs for small and medium scale launchers [1–7]. The use of HREs in launch applications requires the identification of fuel formulations and methods providing sufficiently fast r_f to get high-enough thrust with relatively simple grain geometries [8, 9]. Early HREs conceived for launch applications were based on fuels as hydroxyl-terminated polybutadiene and standard injection methods [10, 11]. These engine configurations required large burning surfaces to provide high thrust levels [11], thus featuring low volumetric efficiency, and high inert masses [10, 11]. Liquefying fuels [12, 13] and non-conventional injection methods (swirl/vortex flow) [14–16] tackle the slow r_f of conventional HRE configurations, while offering the opportunity to work with single, central port grains. This opens new opportunities for the use of the safe and green solid fuels in launch systems. Thanks to the entrainment mass transfer [12, 17–20], liquefying fuels provide r_f resulting 3 to 4 times that achieved by hydroxyl-terminated polybutadiene burning under similar operating conditions [12, 13]. Paraffin-waxes are the most common liquefying fuel and are widely studied. However, paraffin-waxes (and liquefying fuels in general) feature low mechanical and thermal properties. The conventional strategy to enhance the mechanical response of paraffin waxes is their blending with reinforcing polymers [13, 18]. On the other hand, blending has negative effects on the liquefying fuel properties, limiting entrainment mass transfer and, thus, the r_f [20]. Blending with special additives [21] is reported as effective in mitigating wax mechanical properties without compromising entrainment, though thermal behavior of the wax remains a criticality. Non-standard oxidizer injection methods provide augmented r_f for conventional and liquefying formulations, thanks to the enhanced convective heat transfer and mixing promoted by the swirl/vortex flow [15, 16, 22–25]. However, these methods can cause uneven fuel grain consumption due to viscous damping of the oxidizer swirl/vortex flow, particularly in relatively long fuel grains.

Reinforcing strategies other than the blending of wax with polymers are discussed in the literature and reviewed in [26, 27]. In this field, innovative solutions can be achieved thanks to additive manufacturing. The *SPLab* of Politecnico di Milano has developed an original wax reinforcement strategy based on the use of 3D-printed cellular structures [26, 27]. The *armored grain* is a heterogeneous fuel in which wax reinforcement is achieved by a cellular structure embedded in the solid grain. The reinforcing element is an open-cell structure, and its purpose is the provision of mechanical response to the grain.

This study builds on previous advancements by extending lab-scale testing of armored grains and evaluating their performance in terms of r_f. Investigation includes the effects of (i) oxidizer type, (ii) swirl intensity, and (iii) wax composition. The scale-up analysis targets the evaluation of the armored grain in a small-scale test bench. A 400 N HRE designed and implemented by Skyward Experimental Rocketry [28], a student association of Politecnico di Milano.

The presented results are part of the ongoing activities pursued by SPLab toward fuel formulations combining fast regression rates and a general set of suitable properties (in particular, from the mechanical point of view).

2. Methodology

The work targets the evaluation of (i) sustainable waxes, and (ii) scale-up of the armored grain. The work considers different waxes first. Following this preliminary assessment, scaling-up is analysed. Analysis of the scale-up of the armored grain requires considerations on the cellular structure printing at different scales. The topic is fully discussed in Ref. [29], and is briefly revised here.

2.1 Sustainable Waxes

In the analysis, a reference wax is considered. This material serves as baseline for the relative grading of the other waxes. The baseline is a conventional paraffin-wax. The other fuels being derived from sustainable sources. Thermal, and mechanical properties of the waxes are investigated in a pre-burning phase. Following this early step, the reference paraffin wax is used as the main component of fuels that are extensively tested in an armored grain configuration. The reinforcing structure considered in this work is the gyroid [26, 27]. The gyroid is a triply periodical minimum surface, open-cell structure.

2.2 Scaling-up of the Armored Grain

Targeting the testing at different scales, different aspects should be considered. Some of these are related to the HRE testing, and include (but are not limited to) operating parameters as oxidizer to fuel ratio, oxidizer injection conditions, p_c and port size [30]. Other aspects to be considered are related to the gyroid structure, and its properties (in particular, $\tilde{\rho}_{\%}$). For a given relative density, gyroid size (say, cellular structure diameter) and 3D-printer parameter (nozzle orifice diameter) influences the gyroid cell size. Testing at different scales an armored grain requires knowledge of these parameters and of their dependencies. While a strict similarity analysis of the hybrid combustion at different scales is out of the scopes of this work, the evaluation of the ballistic response of different

formulations requires the understanding of the effects of oxidizer composition and injection conditions. The small scale testing of SPLab is typically performed in gaseous oxygen, and with swirled injection [20, 27, 31]. On the other hand the engine designed and implemented by Skyward Experimental Rocketry works with N_2O, and standard injection. Thus, the scale-up analysis requires a preliminary testing in which oxidizer type and injection conditions are clarified at small scale. Additionally, the scale-up analysis requires the identification of printing conditions providing a similarity between the grain diameters and the gyroid cell size.

3. Materials and Methods

In this Section, materials and methods are presented. Base ingredients of the fuels are introduced first, before clarifying formulation nomenclature and classification into *Group 1* and *Group 2*. Finally, for the *Group 2*, additional details concerning the scale-up are detailed.

3.1 Tested materials

Tested materials are hereby presented, together with relevant details on the tested hardware and the implemented data reduction procedures. Based on the methodology presented in Section 2, clarification on the materials and tested formulations is given first. Then, focus moves to the experimental activities.

3.1.1 Paraffin and Bio-derived Waxes

In the analysis, a microcrystalline wax (SasolWax 0907) is used as reference material. The selection of the SasolWax 0907 is related to its wide use in propulsion studies [17, 18, 20, 27, 32]. In addition to this, two waxes from sustainable sources are considered: beeswax (sWB) and carnauba (sWC). While some preliminary work is available on beeswax [33, 34], carnauba is less known as fuel in the HRE community. The wax is produced starting from he leaves of palms belonging to the Copernicia species. In the Table 1, the wax-based fuels are identified in the *Group 1*. As reported in the Section 2, this part of the analysis aims at identifying suitable sustainable candidates for paraffin-wax replacement.

3.1.2 Wax Reinforcement

The armored grain concept is based on the use of a gyroid structure for grain reinforcement. Clarifications on the structure selection, with discussion of detailed references are available in [26, 27]. Basically, the gyroid is selected in the light of its open-cell structure (enabling melted wax to adhere to the printed element), good overall mechanical properties, and fast printing (being a structure commonly implemented in commercial printers). The technique gyroid are printed in is fuse deposition melting. While a variety of materials can be selected for the gyroid printing [26], in this analysis only ABS is considered. This choice is based on (i) high heat deflection temperature of ABS, (ii) strong mechanical properties [26], (iii) good ballistic response of ABS-based armored grains [27], (iv) a single material should be considered to limit the small-/intermediate-scale test number and strategy. Additionally, the formulations featuring a gyroid reinforcement are based on mWP, reinforced by a styrene-based copolymer (SEBS-MA) [18, 20, 26]. These fuel formulations are gathered in the *Group 2* in the Table 1. Such a choice is bounded to the use of the armored grain in the EUROC 2024 Competition [35] by Skyward Experimental Rocketry. Targeting the scale-up of the solution, the *Group 2* includes formulations mWP is blended in. This choice is made to favor the scale-up of the solution, in term of solid fuel manufacturing and handling. Since the small scale testing is based on fuel grains with external diameter of 30 mm, while the grain of the HRE by Skyward Experimental Rocketry features an outer diameter of 75 mm. Under these conditions, considering (i) details of the printing process, (ii) available commercial nozzles for the 3D printer extruder (with orifices ranging from 0.4 to 1.0 mm), an analysis was made measuring the unit cell length of gyroids with outer diameters of 30 and 75 mm. The resulting non-dimensional parameter considered in the analysis is the unit cell length over the external diameter (λ/D_e). Table 2 summarizes the achieved results.

Thus, in the testing at small scale, the effect of λ/D_e is investigated, in a first phase: extruder nozzle diameters of 0.4 mm and 0.8 mm are considered for $\tilde{\rho}$ of 10% and 15%. The upper limit for the extruder nozzle size is determined considering that Skyward Experimental Rocketry implements a gyroid printed with an extruding orifice diameter of 0.8 mm, and $\tilde{\rho}$ = 10%. Table 3 shows details of the tested fuel formulations.

Relative ballistic grading between reference paraffin-wax and sustainable waxes is the main output of tests of *Group 1*. SPLab activities on *Group 2* targets evaluation of the effects, under the investigated conditions, of oxidizer composition and swirl, thus yielding to scale-up of the armored grain with the Skyward testing. Infill and extruding nozzle diameter are chosen so that (i) an evaluation of λ/D_e effects is made at SPLab, (ii) Skyward ER armored grain features a λ/D_e in the range tested at small scale (see Table 2, and Table 3).

3.2 Experimental Methods

The work investigates the pre-burning characteristics of the fuels and of their ingredients, and the burning behavior of the fuels listed in the *Group 1* and *Group 2*.

Table 1. Tested fuel formulations and their composition. In *Group 2*, armored grains are identified by *-i10* and *-i15* suffixes, these indicate the infill of the gyroid structure (10 and 15 $vol.\%$, respectively). Gyroid mass fraction is not reported, being the complement for 100 $wt.\%$ in the armored formulations.

Group	**Fuel ID**	**Composition**	**Density, ρ_f, kg/m^3**
1	W1	mWP (99 $wt.\%$), C (1 $wt.\%$)	929
	B100	sWB (99 $wt.\%$), C (1 $wt.\%$)	905
	C100	sWC (99 $wt.\%$), C (1 $wt.\%$)	996
	B50C50	sWB/sWC (49.5$wt.\%$/49.5$wt.\%$), C(1 $wt.\%$)	947
2	W1S05	mWP (94 $wt.\%$), SEBS-MA (5 $wt.\%$), C (1 $wt.\%$)	929
	W1S10	mWP (94 $wt.\%$), SEBS-MA (5 $wt.\%$), C (1 $wt.\%$)	929
	W1S05-i10	mWP (83.2 $wt.\%$), SEBS-MA (4.4 $wt.\%$), C (0.9 $wt.\%$)	944
	W1S05-i15	mWP (78.0 $wt.\%$), SEBS-MA (4.1 $wt.\%$), C (0.8 $wt.\%$)	951
	W1S10-i10	mWP (78.8 $wt.\%$), SEBS-MA (8.7 $wt.\%$), C (0.9 $wt.\%$)	943

Extruder	**SPLab (D_e = 30 mm)**		**Skyward ER (D_e = 75 mm)**	
Nozzle	$\tilde{\rho}$ = 10 %	$\tilde{\rho}$ = 15 %	$\tilde{\rho}$ = 10%	$\tilde{\rho}$ = 15%
0.4	0.369	0.245	0.147	0.098
0.6	0.557	0.373	0.224	0.149
0.8	0.755	0.502	0.301	0.201
1.0	0.931	0.631	0.378	0.252

Table 2. Gyroid unit cell length over grain external diameter (λ/D_e) as a function of the 3D-printer extruding nozzle orifice size, for relevant $\tilde{\rho}$. In the armored grain scale-up, λ/D_e is considered as a parameter for experimental matrix definition.

Group	Fuel ID	*SPLab*			*Skyward ER*
		O_2		N_2O	N_2O
		Swirl	Axial	Axial	Axial
1	W1	2 | 6 | 5			
	B100	2 | 6 | 5			
	C100	2 | 6 | 5			
	B50C50	3 | 6 | 5			
2	W1S05	2 | 6 | 5	3 | 6 | 5	3 | 6 | 5	2 | 11 | 25
	W1S10	2 | 6 | 5	3 | 6 | 5	3 | 6 | 5	
	W1S05-i10n04	2 | 6.5 | 5	3 | 6 | 5	3 | 6 | 5	
	W1S05-i10n08	3 | 5 | 5	3 | 5 | 5	3 | 5 | 5	
	W1S05-i15n04	3 | 6 | 5	3 | 6 | 5	3 | 6 | 5	
	W1S10-i10n04	2 | 6 | 5	3 | 6 | 5		
	W1S10-i10n08	3 | 6 | 5	3 | 6 | 5		

Table 3. Test matrix. Data shows (i) number of tested samples, (ii) the nominal burning time in s, and (iii) the initial port diameter (in mm). All *SPLab* tests are performed with oxidizer mass flow rate of 5 g/s, while in *Skyward Experimental Rocketry* tests 150 g/s of N_2O are used.

3.2.1 Pre-burning Analyses

Thermal behavior of the tested materials is investigated by simultaneous thermal analyses (DTA-TG). Tests are performed in inert environment (Ar, 75 ml/min) at the heating rate of 10 K/min using a Netzsch STA 449 F5 Jupiter with a vertical weighting system at a pressure of 0.1 MPa. Tested samples have a mass of 15 ± 0.5 mg. The analysis targets the onset/end temperatures for melting and thermal degradation.

Mechanical properties of the tested materials are investigated by compression tests performed on a MTS 810 equipped with a 250 kN load cell, following the ISO 604 standard [36]. At least four samples for each formulation are tested and at least three are used for the analysis of the mechanical properties. The tested samples shape is cylindrical, with a height of 50 mm and a diameter of 30 mm. A key point in the analysis is to avoid buckling of the sample during the compression test (ϵ < 14.4%). The compression rate is set to 1 mm/min. The E and the yield point data (σ_y, and ϵ_y) are the main observables of the analysis.

3.2.2 Burning Analyses

Combustion tests are performed on the SPLab HRE extensively described in Refs. [20, 27]. The test engine implement a swirl injection, with geometrical swirl number of 3.3 [15, 20, 37, 38]. In this work, the effects of swirl are investigated, and this is done considering a different injector plate enabling standard flow. The main observable of interest is the (time-and space-averaged) r_f. This latter parameter is determined by a thickness over time method based on mass balance. Details on the evaluation of the Δt_b evaluation, and on the r_f determination are given in [20, 27]. Burning time of the different formulations is determined based on the expected r_f, with the aim of granting similar values for the time- and space-averaged G_{ox} characterizing the runs.

4. Results and Discussion

4.1 Pre-burning Analyses

4.1.1 Thermal Behavior

Outputs from the simultaneous thermal analyses on the materials are reported in Table 4, where data focus on *Group 1* fuels. The W1 and the C100 show similar $T_{Peak,\,Melting}$. The $T_{Degradation,\,Onset}$ of W1 is the highest, with C100 showing a good thermal resistance. In general, the thermal response of B100 is weaker, with lower melting and degradation onset points than the counterparts. The fuel B50C50 has intermediate characteristics between the pure components blended into it. This latter formulation is investigated based on evidences from the mechanical testing of waxes to balance the stiff and rigid behavior of C100 with B100 (see Subsection 4.1.2). As reported in Refs. [20, 26, 27], the contrasting W1 and W1S05 and W1S10 shows no marked effect on the melting onset and peak temperatures of the SEBS-MA-loaded fuels. On the other hand, for *Group 2* fuels, an effect is noted on the degradation onset temperature, that is drifted toward the styrene-copolymer value, with a temperature increase of $\approx$ 10 K with respect to the non-blended for-

mulation (W1).

4.1.2 Compression Behavior

Compression behavior of the formulations is analysed considering W1 as reference for a normalization, and limiting the printed gyroid analyses to an extruding nozzle of 0.4 mm. Focusing on the *Group 1*, C100 is the fuel with the highest values of all the observable parameters of interest (see Table 5). On the other hand, sWB behaves similarly to macrocrystalline waxes, exhibiting the lowest values for the normalized E and the yield stress, though the yield strain is relatively high. All the waxes feature break at the yield point. The armored grains feature a (desirable) E reduction with respect to the reference wax, and, as detailed in Ref. [26, 27, 39] the absence of an identifiable breakage of the specimen during testing till the ISO 604 limiting values (for the given strand geometry) of 14.4%.

4.2 Burning Behavior

An overview of the results from the burning tests is reported in Table 6. Analysis of *Group 1* results show the close performances of the W1 with the sustainable counterparts. The fastest r_f is the one of B100. C100 and B50C50 exhibit similar performances with respect to W1. This is in particular true for the blended formulation, whose r_f performance, under the investigated conditions, is overlapped to the one of the paraffin-wax. Under the investigated conditions, *Group 2* results for tests in O_2 show a limited impact of the swirl injection, while a significant r_f impact is due to the use of the armored grain. In particular, independently from the gyroid infill, armored grains based on W1S5 feature faster r_f than the non-armored counterpart. The result is even more relevant when considering that, for example, W1S05-i10n04 exhibits a percent r_f increase over W1S05 of nearly 30%, in spite of a lower $\bar{G_{ox}}$ (29 kg/m^2s vs. 48 kg/m^2s). Considering swirl effects, the non-armored formulations show faint (if any) r_f increases over the axial injection case. A small difference is noted for the W1S05-i10n08, the fastest fuel in the dataset. For this fuel, the relatively high λ/D_e seems to provide higher performance in the axial injection case. While this result requires further investigations, it could be promising in the light of a fuel grain configuration granting fast regression rates with conventional standard methods. Contrasting the combustion tests with axial injection, the variation of the oxidizer from O_2 to N_2O shows minor effects on the relative grading of the fuels. Such a result is likely due to the relatively low $\bar{G_{ox}}$ range considered in the analysis [40].

Fig. 1, and Fig. 2 show the data recorded in one of the two Skyward Experimental Rocketry firings, and a picture of the engine plume, respectively. Data in Fig. 1 are N_2O injector pressure, pre- and post-combustion chamber pressures. Overall the collected data show a relatively stable behavior of the engine during the firing. A direct comparison between the small scale testing and the firing with the Skyward Experimental Rocketry HRE is complicated also due to the differences in the operating conditions implying liquid oxidizer injection in the scale-up tests. In spite of this, from the $r_f = a_r \cdot G_{ox}^{n_r}$ presented in Ref. [27] for W1S05, and extrapolating the data from tests in O_2 with swirl injection to the condition tested in Skyward Experimental Rocketry HRE (see Table 6), the achieved regression rate of the armored grain scale-up feature a percent increase over expectations in the range 10 to 15%. The result deserves further analyses and shows the applicability of the armored grain to relatively large systems.

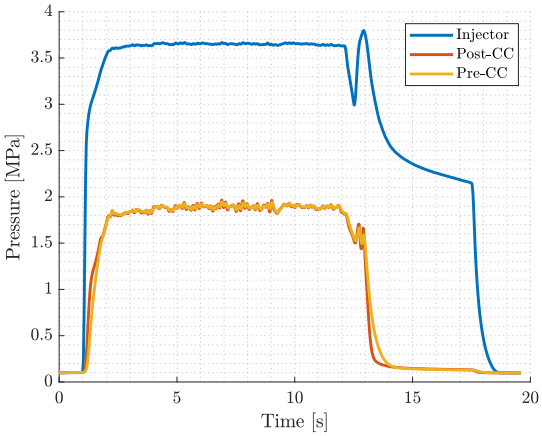

Fig. 1. Data acquired during one of the armored grain tests in Skyward ER HRE: pressure traces on the injector housing, pre- and post-combustion chambers.

5. Conclusions

The presented work is a snapshot of the current activities ongoing at *SPLab* in the frame of the development of solid fuel formulations for hybrid propulsion. The activities target the development of more sustainable, green and safe propulsion systems. The presented analysis focuses on the armored grain concept, and present some pre-burning and combustion analyses of waxes from sustainable sources. The armored grain is here scaled-up in a 400 N-class HRE property of Skyward Experimental Rocketry, a student association of Politecnico di Milano. Experimental testing is performed at small scale, to provide a relative ballistic grading of different fuels to provide also a better insights of the armored grain features. In this phase, tackled effects are (i) the wax type (paraffin- vs. sustainable waxes), (ii) the injection implementation

Table 4. Thermal analysis results of paraffin and natural axes of *Group 1* (300 K < T < 873 K).

Specimen	$T_{Melting,\,Onset}$	$T_{Melting,\,Peak}$	$T_{Degradation,\,Onset}$	Δm @ 873 K
W1	326	359	689	-99.9
B100	331	340	584	-99.9
C100	353	361	669	≈ -100
B50C50	341	357	622	-97.0

Table 5. Mechanical properties at compression of the investigated waxes (compression rate 1 mm/min, testing temperature 293 ± 3 K). Data are normalized with W1 as reference.

Group	**Specimen**	**Normalized Young Modulus**, E_{Fuel}/E_{W1}	**Normalized Yield Stress**, $\sigma_{Fuel,\,\mathrm{y}}/\sigma_{W1,\,\mathrm{y}}$	**Normalized Yield Strain**, $\epsilon_{Fuel,\,\mathrm{y}}/\epsilon_{W1,\,\mathrm{y}}$
1	W1	1.0	1.0	1.0
	B100	0.2	0.3	2.4
	C100	2.8	4.3	1.2
	B50C50	1.6	2.1	1.1
2	W1S05	1.3	1.3	0.9
	W1S10	1.2	1.4	1.3
	W1S05-i10	0.8	0.9	1.1
	W1S05-i15	0.6	0.9	2.5
	W1S10-i10	N.Av.	N.Av.	N.Av.

Fig. 2. Exhaust plume picture captured by Skyward Experimental Rocketry Team.

effects (swirl vs. axial) and (iii) the effects of the oxidizer (O_2 vs. N_2O). Under the investigated conditions, waxes from sustainable sources, and in particular sWC and its blend with sWB yielded fuel formulations whose ballistic performance is similar to the one of the baseline paraffin-wax. This opens new opportunities for the analysis of innovative fuels. Focusing on the relative ballistic grading targeting the armored grain scale-up, under the investigated conditions swirl exhibited only minor effects on the r_f. This is likely due to the relatively low swirl number, and swirl decay. The passage from O_2 to N_2O, at small scale yielded minor effects too. This is due to the relatively low G_{ox} characterizing the *SPLab* test bench, and the gaseous injection condition met for both the oxidizers. The armored grain W1S05-i10n08, when tested at small scale showed the best performances in terms of r_f, and a ballistic response showing better results in axial injection than in swirl flow. This point requires future investigations to extend the testing conditions and to understand the (possible) role of the gyroid in the regression rate enhancement. On the other hand, W1S05-i10n08 when scaled-up showed a relatively stable combustion, showing the possible implementation of the armored grain concept at larger scales.

Acknowledgements

This activity has been performed within the MUSA – Multilayered Urban Sustainability Action – project, funded by the European Union – NextGenerationEU, under the National Recovery and Resilience Plan (NRRP) Mission 4 Component 2 Investment Line 1.5: Strengthening of research structures and creation of $R\&D$ "innovation ecosystems", set up of "territorial leaders in $R\&D$".

Group	**Fuel ID**	**Average oxidizer mass flux** $\bar{G_{ox}}, kg/m^2s$	**Regression rate** $\bar{r_f}, mm/s$
1	W1	36.3 ± 1.4	1.21 ± 0.04
	B100	33.8 ± 1.5	1.41 ± 0.04
	C100	43.2 ± 2.5	1.18 ± 0.09
	B50C50	37.4 ± 1.1	1.26 ± 0.04
SPLab, Swirl, O_2			
2	W1S05	48.35 ± 0.42	1.25 ± 0.05
	W1S10	58.56 ± 0.76	1.04 ± 0.03
	W1S05-i10n04	28.85 ± 0.99	1.64 ± 0.14
	W1S05-i15n04	32.98 ± 2.05	1.60 ± 0.06
	W1S05-i10n08	28.95 ± 0.81	2.01 ± 0.08
	W1S10-i10n04	34.18 ± 0.44	1.56 ± 0.09
	W1S10-i10n08	32.91 ± 1.84	1.61 ± 0.07
SPLab, Axial, O_2			
2	W1S05	50.74 ± 1.84	1.24 ± 0.02
	W1S10	57.21 ± 2.26	1.01 ± 0.02
	W1S05-i10n04	26.73 ± 0.20	1.83 ± 0.07
	W1S05-i15n04	29.52 ± 1.75	1.81 ± 0.11
	W1S05-i10n08	31.64 ± 0.52	1.96 ± 0.09
	W1S10-i10n04	34.40 ± 2.22	1.54 ± 0.04
	W1S10-i10n08	30.82 ± 0.52	1.59 ± 0.06
SPLab, Axial, N_2O			
2	W1S05	53.13 ± 1.94	1.22 ± 0.11
	W1S10	65.57 ± 0.04	1.00 ± 0.00
	W1S05-i10n04	31.82 ± 1.62	1.82 ± 0.10
	W1S05-i15n04	35.12 ± 3.17	1.57 ± 0.05
	W1S05-i10n08	32.08 ± 1.61	2.10 ± 0.08
Skyward ER, Axial, N_2O			
2	W1S05-i10n08	91.38±2.75	1.64±0.13

Table 6. Regression rate data for the tested formulations.

The collaboration and the professional skills of the students of Skyward Experimental Rocketry were highly appreciated throughout the work.

References

[1] Blue Shift Aerospace, *Blue shift aerospace (website)*, https://www.blushiftaerospace.com/, Accessed: 2024-09-03.

[2] Gilmour Space, *Gilmour space (website)*, https://www.gspace.com/, Accessed: 2024-09-03.

[3] HyImpulse, *Hyimpulse technologies (website)*, https://www.hyimpulse.de/en/, Accessed: 2024-09-03.

[4] Innospace, *Innospace (website)*, https://www.innospc.com/, Accessed: 2024-09-03.

[5] SpaceZone India, *Spacezone india (website)*, https://www.spacezoneindia.com/, Accessed: 2024-09-03.

[6] TiSpace, *Tispace (website)*, https://tispace.com/en, Accessed: 2024-09-03.

[7] Vaya Space, *Vaya space - the future of space launch and defense propulsion (website)*, https://www.vayaspace.com/, Accessed: 2024-09-03.

[8] C. Glaser, J. Hijlkema, and J. Anthoine, "Bridging the technology gap: Strategies for hybrid rocket engines," *Aerospace*, vol. 10, no. 10, 2023, ISSN: 2226-4310. DOI: 10.3390/aerospace10100901. [Online]. Available: https://www.mdpi.com/2226-4310/10/10/901.

[9] M. Stella *et al.*, "Experimental investigation of a h2o2 hybrid rocket with different swirl injections and fuels," *Applied Sciences*, vol. 14, no. 13, 2024, ISSN: 2076-3417. DOI: 10.3390/app14135625. [Online]. Available: https://www.mdpi.com/2076-3417/14/13/5625.

[10] D. Altman and A. Holzman, "Overview and history of hybrid rocket propulsion," in *Fundamentals of hybrid rocket combustion and propulsion*, M. J. Chiaverini and K. K. Kuo, Eds., American Institute of Aeronautics and Astronautics, 2007, ch. 1. DOI: 10.2514/5.9781600866876.0001.0036.

[11] G. Story, "Large-scale hybrid motor testing," in *Fundamentals of hybrid rocket combustion and propulsion*, M. J. Chiaverini and K. K. Kuo, Eds., American Institute of Aeronautics and Astronautics, 2007, ch. 13, pp. 513–552. DOI: 10.2514/5.9781600866876.0513.0552. eprint: https://arc.aiaa.org/doi/pdf/10.2514/5.9781600866876.0413.0456. [Online]. Available: https://arc.aiaa.org/doi/abs/10.2514/5.9781600866876.0413.0456.

[12] M. Karabeyoglu, D. Altman, and B. J. Cantwell, "Combustion of liquefying hybrid propellants: Part 1, general theory," *Journal of Propulsion and Power*, vol. 18, no. 3, pp. 610–620, 2002. DOI: 10.2514/2.5975.

[13] K. Veale, S. Adali, J. Pitot, and M. Brooks, "A review of the performance and structural considerations of paraffin wax hybrid rocket fuels with additives," *Acta Astronautica*, no. 141, pp. 196–208, 2017. DOI: 10.1016/j.actaastro.2017.10.012.

[14] C. Lee, Y. Na, and G. Lee, "The enhancement of regression rate of hybrid rocket fuel by helical grain configuration and swirl flow," in *41st AIAA/ASME/SAE/ASEE Joint Propulsion Conference & Exhibit, Tucson, AZ, USA*, 10-13 July 2005. DOI: 10.2514/6.2005-3906.

[15] Y. Saburo, S. Noriko, and H. Kousuke, "Controlling parameters for fuel regression rate of swirling-oxidizer-flow-type hybrid rocket engine," in *48th AIAA/ASME/SAE/ASEE Joint Propulsion Conference & Exhibit, Atlanta, GA, USA*, 30 July-1 August 2012. DOI: 10.2514/6.2012-4106.

[16] M. Franco *et al.*, "Regression rate design tailoring through vortex injection in hybrid rocket motors," *J. Spacecr. Rockets*, vol. 57, pp. 278–290, 2020. DOI: 10.2514/1.A34539.

[17] M. Kobald, C. Schmierer, H. Ciezki, S. Schlechtriem, E. Toson, and L. De Luca, "Evaluation of paraffin-based fuels for hybrid rocket engines," 50th AIAA/ASME/ SAE/ASEE Jt. Propuls. Conf, 2014, pp. 1–14. DOI: 10.2514/6.2014-3646.

[18] C. Paravan, L. Galfetti, and F. Maggi, "A critical analysis of paraffin-based fuel formulations for hybrid rocket propulsion," in *53rd AIAA/SAE/ASEE Joint Propulsion Conference*, AIAA Paper No. 2017-4830, 2017. DOI: 10.2514/6.2017-4830.

[19] Y. Tang, S. Chen, W. Zhang, R. Shen, L. T. DeLuca, and Y. Ye, "Mechanical modifications of paraffin-based fuels and the effects on combustion performance," *Propellants Explos. Pyrotech.*, vol. 42, pp. 1268–1277, 2017. DOI: 10.1002/prep.201700136.

[20] C. Paravan, L. Galfetti, R. Bisin, and F. Piscaglia, "Combustion processes in hybrid rockets," *International Journal of Energetic Materials and Chemical Propulsion*, vol. 18, no. 3, 2019. DOI: 10.1615/IntJEnergeticMaterialsChemProp.2019027834.

[21] K. Bilge, U. Kokal, N. B. Emerce, U. C. Yildiz, M. Baysal, and A. Karabeyoglu, "Selection criteria for tackifier addition to paraffin wax based hybrid rocket fuels," in *AIAA Propulsion and Energy 2019 Forum*, 2019, pp. 1–14. DOI: 10.2514/6.2019-3921.

[22] C. P. Kumar and A. Kumar, "Effect of swirl on the regression rate in hybrid rocket motors," *Aerosp. Sci. Technol.*, vol. 29, pp. 92–99, 2013. DOI: 10.1016/j.ast.2013.01.011.

[23] R. Sakote, N. Yadav, S. Karmakar, P. C. Joshi, and A. K. Chatterjee, "Regression rate studies of paraffin wax-htpb hybrid fuels using swirl injectors," *Propellants Explos. Pyrotech.*, vol. 39, pp. 859–865, 2014. DOI: 10.1002/prep.201300207.

[24] E. Paccagnella, F. Barato, D. Pavarin, and A. Karabeyoğlu, "Scaling parameters of swirling oxidizer injection in hybrid rocket motors," *J. Propuls. Power*, vol. 33, pp. 1378–1394, 2017. DOI: 10.2514/1.B36241.

[25] F. D. Quadros and P. T. Lacava, "Swirl injection of gaseous oxygen in a lab-scale paraffin hybrid rocket motor," *J. Propuls. Power*, vol. 35, pp. 896–905, 2019. DOI: 10.2514/1.B37283.

[26] R. Bisin, C. Paravan, S. Alberti, and L. Galfetti, "A new strategy for the reinforcement of paraffin-based fuels based on cellular structures: The armored grain—mechanical characterization," *Acta Astronautica*, vol. 176, pp. 494–509, 2020. DOI: 10.1016/j.actaastro.2020.07.003.

[27] R. Bisin and C. Paravan, "A new strategy for the reinforcement of paraffin-based fuels based on cellular structures: The armored grain — ballistic characterization," *Acta Astronautica*, vol. 206, pp. 284–298, 2023, ISSN: 0094-5765. DOI: https://doi.org/10.1016/j.actaastro.2023.02.027.

[28] Skyward Experimental Rocketry, *Skyward experimental rocketry (website)*, https://www.skywarder.eu/, Accessed: 2024-09-19.

[29] A. Garcidueñas Correa, "Cellular structures as reinforcing strategy in paraffin-based fuels for hre: Oxidizer, injection and grain scale-up effects," *MSc Dissertation in Aerospace Engineering, Politecnico di Milano*, 2023. [Online]. Available: https://hdl.handle.net/10589/213999.

[30] A. Gany, "Similarity and scaling effects in hybrid rocket motors," in *Fundamentals of hybrid rocket combustion and propulsion*, M. J. Chiaverini and K. K. Kuo, Eds., American Institute of Aeronautics and Astronautics, 2007, ch. 12. DOI: 10.2514/5.9781600866876.0489.0512.

[31] C. Paravan, "Nano-sized and mechanically activated composites: Perspectives for enhanced mass burning rate in aluminized solid fuels for hybrid rocket propulsion," *Aerospace*, vol. 12, no. 6, pp. 1–31, 2019, ISSN: 2226-4310. DOI: https://doi.org/10.3390/aerospace6120127.

[32] M. Grosse, "Effect of a diaphragm on performance and fuel regression of a laboratory scale hybrid rocket motor using nitrous oxide and paraffin," in *45th AIAA/ASME/SAE/ASEE Joint Propulsion Conference & Exhibit*, AIAA Paper No. 2009-5113, 2009. DOI: https://doi.org/10.2514/6.2009-5113.

[33] V. I. Naoumov, H. Nguyen, and B. Alcalde, "Study of the combustion of beeswax and beeswax with aluminum powder in hybrid propellant rocket engine," in *54th AIAA Aerospace Sciences Meeting*. DOI: 10.2514/6.2016-2145. eprint: https://arc.aiaa.org/doi/pdf/10.2514/6.2016-2145. [Online]. Available: https://arc.aiaa.org/doi/abs/10.2514/6.2016-2145.

[34] K. J. Stober, R. M. M. Apodaca, and D. Wood, "Paraffin & beeswax spaceflight experiments for improved understanding of centrifugal casting," in *2022 IEEE Aerospace Conference (AERO)*, 2022, pp. 1–8. DOI: 10.1109/AERO53065.2022.9843648.

[35] EuRoC, *European rocket competition (website)*, https://www.euroc.pt/, Accessed: 2024-09-03.

[36] *Iso-604 standard (2003)*, https://www.iso.org/standard/31261.html, Last accessed: 2022-03-03, 2003.

[37] J. Messineo, K. Kitagawa, C. Carmicino, T. Shimada, and C. Paravan, "Reconstructed ballistic data versus wax regression-rate intrusive measurement in a hybrid rocket," *Journal of Spacecraft and Rockets*, vol. 57, no. 6, pp. 1295–1308, 2020. DOI: 10.2514/1.A34695. eprint: https://doi.org/10.2514/1.A34695. [Online]. Available: https://doi.org/10.2514/1.A34695.

[38] M. T. Migliorino *et al.*, "Numerical and experimental analysis of fuel regression rate in a lab-scale hybrid rocket engine with swirl injection," *Aerospace Science and Technology*, vol. 140, p. 108 467, 2023, ISSN: 1270-9638. DOI: https://doi.org/10.1016/j.ast.2023.108467. [Online]. Available: https://www.sciencedirect.com/science/article/pii/S1270963823003644.

[39] C. Paravan, F. Giambelli, and R. Bisin, "Paraffin-based fuels: Perspectives from different reinforcing strategies and metal additives," in *13th International Symposium on Special Topics in Chemical Propulsion (ISICP), Gjøvik , Norway*, 31 May-2 June 2023.

[40] L.-l. Liu, X. He, Y. Wang, Z.-b. Chen, and Q. Guo, "Regression rate of paraffin-based fuels in hybrid rocket motor," *Aerospace Science and Technology*, vol. 107, p. 106 269, Dec. 2020, ISSN: 1270-9638. DOI: 10.1016/j.ast.2020.106269. [Online]. Available: http://dx.doi.org/10.1016/j.ast.2020.106269.